Energy & Buildings 350 (2026) 116646

Contents lists available at ScienceDirect

Energy & Buildings

journal homepage: www.elsevier.com/locate/enb

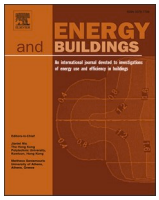

Experimental investigations of internal macro-scale convection in the loose-fill wood fiber insulation layer of a full-scale wall element

Martin Veit [a,b,c,*], Hicham Johra [a,d], Nikolaj Rask [a], Simon M. Roesgaard [a], Rasmus Lund Jensen [a]

[a] Department of the Built Environment, Aalborg University, Thomas Manns Vej 23, 9220 Aalborg, Denmark
[b] Slovenian National Building and Civil Engineering Institute (ZAG), Department for Research of Fire-Safe Sustainable Built Environment (FRISSBE), Obrtna cona Logatec, 1370, Slovenia
[c] Ghent University, Department of Structural Engineering and Building Materials, Technologiepark-Zwijnaarde 60, 9052 Gent, Belgium
[d] SINTEF Community, Department of Architectural Engineering, Børrestuveien 3, 0373 Oslo, Norway

ARTICLE INFO

Keywords:
Laboratory measurements
Guarded hotbox method
Internal macro-scale convection
Heat transfer
Insulation
Loose-fill
Wood fiber insulation

ABSTRACT

With increasing restrictions on the energy efficiency of buildings, thicker insulation layers are installed in new and refurbished buildings to reduce heat losses. Previous studies have indicated that internal macro-scale convection cells can occur in thick porous insulation layers, decreasing the thermal performance of the envelope component. The focus of previous studies has been on horizontal insulation layers, most often composed of glass wool. Therefore, there is a lack of empirical data for loose-fill insulation and, in particular, bio-based materials, which have the potential of being more sustainable than conventional ones. The present investigation of this paper looks at the possibility of internal macro-scale convection inside loose-fill wood fiber insulation in a full-scale vertical wall element, with the modified Rayleigh number in the current investigation being between 20 and 45 and exhibiting internal convection in all cases. The experimental results show good agreement in terms of heat flux and temperature distribution with numerical simulations where the macro-scale convection is modelled explicitly. It also indicates that internal macro-scale convection can be modelled with existing building physics simulation tools, such as COMSOL. Finally, the internal macro-scale convection increases the effective U-value by up to 90 % for the highest temperature difference in steady-state conditions. This effect appears to diminish under dynamic boundary conditions, with a calculated effective U-value being within the uncertainty of the steady-state case with the lowest temperature difference, indicating that it might be less influential under real conditions.

1. Introduction

Buildings account for 40 % of the total energy demand in the world, and are, therefore, a significant contributor to the emission of greenhouse gases [1]. One option to tackle this issue is to reduce the need for space heating and cooling, by optimizing the thermal performance of the building envelope, for which a better understanding of the mechanisms and dynamic performance of the construction elements is needed if we are to create better envelopes for both new and renovated buildings.

Currently, the assessment of a construction element's thermal performance relies on a theoretical calculation that does not consider certain complex dynamic effects, such as 2D and 3D phenomena in porous insulation layers. A better understanding of building physics is thus needed to bridge the performance gap between measured and computer energy performance in the building sector [2]. Specifically, the case with internal macro-scale internal convection inside loose-fill insulation has not been studied extensively in the literature, despite blown insulation having the advantage of being easily employable for refurbishing wall cavities and attics.

1.1. Performance gap and effective U-value

One cause for the deviation between the calculated and actual energy performance of a building may be due to incomplete characterization of the material properties, especially with the properties and their interaction with real-life weather conditions. This is referred to as the "effective U-value", which is a way of correcting the steady-state

* Corresponding author.
E-mail address: martin.veit@ugent.be (M. Veit).

https://doi.org/10.1016/j.enbuild.2025.116646
Received 7 July 2025; Received in revised form 9 October 2025; Accepted 26 October 2025
Available online 28 October 2025

Nomenclature

A	Area perpendicular to heat flux (m^2)
c_p	Specific heat capacity of air(J kg^{-1} K^{-1})
d	Characteristic length (m)
g	Acceleration due to gravity (m s^{-2})
K	Effective air permeability of insulation (m^2)
$Nu + 1$	Non-dimensional Nusselt number (–)
Q_j	J^{th} measurement of the added power (W)
ΔT	Temperature difference (K)
$\Delta T_{experiment}$	Temperature difference between indoor and outdoor (°C)
$T_{dimensionless}$	Dimensionless temperature (–)
$T_{measured}$	Measured temperature (°C)
T_{ne}	Exterior temperature (°C)
$T_{ne,j}$	J^{th} measurement of the exterior environmental temperature (°C)
T_{ni}	Interior temperature (°C)
$T_{ni,j}$	J^{th} measurement of the interior environmental temperature (°C)
$T_{1D\ heat\ transfer}$	Temperature in point, based on DS 418 calculation (°C)
U	Thermal transmittance (W m^{-2} K^{-1})
β	Thermal expansion coefficient of air (K^{-1})
λ	Thermal conductivity of the insulation (W m^{-1} K^{-1})
υ	Kinematic viscosity of air (m^2 s^{-1})
ρ	Density of air(kg m^{-3})
φ	Heat flux through specimen (W)
φ_{total}	Total heat losses (W)
φ_{cond}	Conductive heat losses (W)

properties to better reflect the actual performance under realistic conditions. A study [3] from Newcastle, Australia, concludes that the thermal resistance (R-value) obtained in steady-state conditions is insufficient to characterize the thermal performance of a construction element. It highlights the thermal mass as a critical parameter to determine the energy performance in realistic conditions and attributes the deviation between steady-state measured U-values and the effective U-value to the thermal mass.

Veit et al. (2023a) [4] investigated the difference in numerically calculated heat losses between steady-state and dynamic calculations for glass wool, mineral wool, and wood fiber insulation. It was found that significant deviations can occur between steady-state and dynamic simulations when looking at heat transfer on a single surface, supported by [5]. However, it concluded that the deviation diminishes when aggregating results over an entire building.

The study did not include 2D effects, such as the phenomenon of internal macro-scale convection inside the insulation layer, which could be why the effects are not more notable when aggregated on the building level. The study further concludes that more work should be done to investigate the 2D effects in more depth, as this can increase the calculated heat losses when including more accurate modelling approaches [6]. Consequently, this study experimentally investigates the effect of internal macro-scale convection on the thermal performance of a full-scale construction element.

1.2. Internal macro-scale convection inside an insulation layer

In Denmark, the heat transfer calculation is based on the national standard DS 418 [7]. The standard thoroughly describes the procedure for determining transmission loss in construction elements. However, there is a lack of guidance for how to consider heat transfer by convection in fibrous insulation materials.

Bankvall [8] extensively investigated how convection, conduction, and radiation affected heat transfer, from which standards have been developed to determine how this should be considered in a building context. The European Standard DS/EN ISO 10456 [9] describes how and when to take internal macro-scale convection into account. The standard proposes the modified Rayleigh number as a measure for the onset of internal macro-scale convection and is determined by equation (1).

$$Ra_m = \frac{g\beta\rho c_p}{\nu}\cdot\frac{dK\Delta T}{\lambda} \tag{1}$$

Where g is the acceleration due to gravity, β is the thermal expansion coefficient of air, ρ is the density of air, c_p is the specific heat capacity for air, υ is the kinematic viscosity of air, ΔT is the temperature difference across the insulation layer, d is the characteristic length scale, K is the effective air permeability of the insulation, and λ is the thermal conductivity of the insulation. As evident by the equation, the internal macro-scale convection is dependent on the temperature gradient across the material, the thickness, and the air permeability of the material.

If corrections are to be made, the standard provides methods to adjust the heat transfer for the temperature and moisture of the material. However, no corrections for insulation are provided, and, therefore, there is not a clear path to implementing this in the building industry. This further emphasizes the view of Wilkes & Rucker (1983) [10], calling for a standardized testing procedure.

Furthermore, the non-dimensional Nusselt number is used to quantify the effect of internal macro-scale convection and is determined as the ratio between convective and conductive heat transfers. It is commonly modified and denoted as Nu + 1 [11] to represent the ratio between the total heat transfer, ϕ_{total}, and the conductive heat transfer, ϕ_{cond}, as shown in equation (2).

$$\mathrm{Nu} + 1 = \frac{\phi_{total}}{\phi_{conductive}} \tag{2}$$

The modified Nusselt number, Nu + 1, is convenient to use since it is unity when no internal macro-scale convection is present.

An explicit standard for testing for internal macro-scale convection and some general method for correcting is still missing in the building industry [7,9]. However, the calculation procedure is difficult to generalize as the convection intensity is highly dependent on the fiber texture, pore structure, and pore tortuosity of each insulation product [12].

The study of internal macro-scale convection in insulation materials is not a new matter. However, the previous efforts have mainly focused on horizontal insulation [13–22], especially attic configurations, as attics are commonly re-insulated with blown fibers for renovation.

The phenomenon of internal macro-scale convection in insulation layers considers air movement inside the pore network of the insulation, driven by the thermal buoyancy of the air. The air close to the warm side of the insulation will be moved upwards, while the air closest to the cold side will be driven downwards (see Fig. 1).

Fiberglass wool in attics has been studied experimentally and numerically. The study [10] investigates both insulation batts and loose-fill, and revealed that the batts behaved as expected, meaning that it is possible to model the thermal performance using the material's thermal properties measured in a small-scale setup in which no macro-convection cell can occur, like the guarded hot plate or the heat flow meter method. However, this was not the case with the loose-fill insulation. The thermal performance exhibited a more complex behavior attributed to internal macro-scale convection inside the loose-fill insulation under winter conditions with significant temperature gradients.

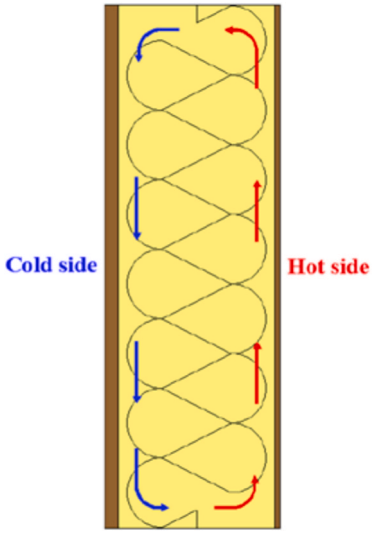

Fig. 1. Illustration of the phenomenon of internal macro-scale convection in porous insulation materials.

However, the study states that the effect on the overall thermal performance of the building is relatively small. The more negligible effect was ascribed to the horizontal orientation of the study case. It was concluded that more work should be put into making a standardized testing procedure based on large-scale setup [10].

Therefore, in recent years, attention has also been directed at internal macro-scale convection phenomena in the vertical insulation layer of wall elements. Experimental and numerical investigations of glass fiber insulation batts test different configurations of boundary conditions with insulation thicknesses of 0.31–0.34 m. The investigation showed an increase of in the heat loss 30 % for a temperature gradient of 20 °C, and an increase of 90 % for a temperature gradient of 40 °C, compared to tests with impermeable boundary conditions. [11] The increased heat loss was assumed to come from air leakages, which could introduce significant internal macro-scale convection and additional heat loss with air movement inside the insulation [23,24].

Gulbrekken et al. [25] investigated a vertical wall element equipped with 500 mm glass wool batts, and the authors found that internal macro-scale convection has a more pronounced effect in vertical insulation layers compared to horizontal ones. The experiment used a rotatable guarded hot box with a metering area of 2450 mm x 2450 mm. The use of the dimensionless Nusselt and Rayleigh numbers indicated the presence of internal macro-scale convection. A Nusselt number of 1.15 was found for vertical measurements, compared to a Nusselt number of 1.09 for horizontal measurements, with a temperature difference of 40 °C. Additionally, the study found that the Nusselt number also increased when the Rayleigh number increased, indicating a correlation between internal macro-scale convection probability and the observed heat transfer by convection. The study found non-linear temperature distributions, as other studies also found.

The effect of internal macro-scale convection for 250 mm and 400 mm of mineral wool batten and wood fiber batten, respectively, has been investigated in [26]. The study used the same setup with the rotatable guarded hot box as in [25]. They concluded that, even though wood fiber batts had a higher Rayleigh number due to higher gas permeability, the mineral wool resulted in a higher Nusselt number. The study attributed the improved performance of wood fiber to its ability to fill out the cavity more efficiently. Table 1..

Dyrbøl et al. [27] investigated internal convection in three different insulation materials with different permeabilities, at different inclinations and different temperature differences. From the experimental campaign, the found an increase in the total heat losses of up to 17 %. Wahlgren et al. [28] investigated loose-fill fiberglass insulation on an attic, both experimentally and numerically, showing that the thermal resistance decreased by 25 % for the experiments and 22 % for the simulations, at a modified Rayleigh number of 35. In a later study, Wahlgren concludes that the critical Rayleigh number for attic configurations are between 10 and 30 [29]. Ciucasu et al. [30] investigated internal convection in loose-fill glass wool insulation, with an open attic configuration with air movement, taking into account the trusses and joints, and concluding that the critical Rayleigh number is in the range of 26 to 28 for the attic configuration, with a Nusselt number of up to 1.7 for modified Rayleigh numbers of 45 for both experimental and simulation results. Similarly, Kivioja et al. [31] investigated the internal convection in loose-fill glass wool in an attic configuration, for different thicknesses and with and without trusses, resulting in 24 case studies. They found an increase in the total heat losses of more than 60 % when the insulation thickness was 600 mm and with forced air flow above the insulation.

Table 1
Material properties of the loose-fill wood fiber insulation in the full-scale experimental setup of the current study.

Density [kg m^{-3}]	Thermal conductivity [W m^{-1} K^{-1}]	Specific heat capacity [J kg^{-1} K^{-1}]	Effective air permeability [m^2]	Relative gas diffusivity [–]
43.42	0.0382	1950	$1.551 \cdot 10^{-9}$	0.557

Additionally, the focus has been on traditional insulation materials like glass wools. However, bio-based insulation materials, such as wood fiber insulation, are relatively new in the building industry, and are far from being thoroughly tested. Furthermore, the work on vertical wall constructions includes insulation materials consisting of batts. The industry uses batts more often compared to loose-fill insulation since problems with subsidence in some loose-fill insulation materials are often experienced [32]. However, this problem does not exist for loose-fill insulation consisting of wood fiber [33]. Therefore, it is of great interest to test internal macro-scale convection in a vertical construction element filled with loose-fill wood fiber insulation.

1.3. Novelty and contribution of the current study

The novelty of this study is in the contribution of more experimental data on full-scale vertical wall elements, along with investigating a bio-based loose-fill wood fiber insulation material, as previous studies have focused on attics and primarily on glass wool or mineral wool. The experimentally obtained data is also seldom compared to numerical models.

A total of 7 distinct steady-state experiment cases and 4 distinct dynamic experiment cases have been performed. The temperature stabilization time of each steady-state case is around 3–4 days, before the measurement period begins. This amounts to up to 21 days of continuous use of the guarded hotbox. For the dynamic cases, it took around 5 days of stabilization before the condition in the wall element reached quasi-steady state, amounting to 20 days of experiment. The number of sensors used provides a high-resolution temperature distribution inside the insulation.

Furthermore, the internal macro convection inside insulation materials is usually investigated with steady-state boundary conditions, which is the worst-case scenario due to the fully developed internal macro-scale convection, but the easiest to perform. However, real-life situations are dynamic. With the addition of dynamic experiments, the phenomenon of internal macro-scale convection can be investigated in more realistic conditions, which has not been investigated before, to the best of the authors' knowledge.

Finally, it has been thoroughly established in the literature that internal macro-scale convection occurs, but the effects on the effective U-value are less documented. Therefore, observing the effects of internal macro-scale convection on insulation materials will shed more light on

the building physics at play, which can help reduce the performance gap between the building performance simulations and the actual thermal performance of real buildings.

This study aims to clarify the relationship between the internal macro-scale convection and the effective U-value, to see its effect on a bio-based loose-fill wood fiber insulation material. Furthermore, the effect is investigated both in steady state and dynamic conditions, as studies have shown that there can be a deviation between the two conditions.

The description of sensor locations of the current study is given in [34]. All empirical data produced by this study are available in open access at [35]. A complete description of the experimental setup is given in [36].

2. Study case description

2.1. Insulation material

The material under investigation is a loose-fill wood fiber insulation, which differs from conventional insulation materials, such as glass wool or mineral wool. Wood fiber is an organic material with higher specific heat capacity, different hygrothermal properties, and more [37]. Since it is a loose-fill insulation material, the material has to be blown into the construction element, making it difficult to achieve a specific density repeatably.

The density of the blown wood fiber insulation layer within the experimental setup is determined from the ratio of the total mass of the insulation to its calculated volume. In this evaluation, the volumes occupied by the joists as well as the effective thickness of the insulation layer are explicitly accounted for to ensure an accurate estimation of the total insulation volume.

The reference heat transfer by conduction alone, excluding any contribution from internal convection, is computed using the thermal conductivity of the insulation under non-convective conditions. This parameter is derived from Guarded Hot Plate (GHP) measurements performed on the same insulation materials as those employed in the test setup. The GHP experiments are conducted under steady-state conditions using top-heated cubic specimens (50 × 50 × 12 cm) at mean temperatures of 10 °C, 25 °C, and 40 °C, with an applied temperature difference of 15 K, utilizing a Guarded Hot Plate apparatus (EP500) [38].

Under these conditions, the GHP method ensures Rayleigh numbers in the range $0.5 < Ra < 1.3$. These values are below both theoretical and experimental critical thresholds for the onset of internal convection. It can therefore be confidently concluded that the effective thermal conductivity values obtained from the GHP measurements represent purely conductive heat transfer, free from any influence of internal convection phenomena.

The heat conductivity of the loose-fill wood fiber insulation, along with common insulation materials and bio-based materials, can be seen as a function of the density in Fig. 2.

The effective air permeability of the wood fiber insulation materials is determined using a *meso*-scale horizontal air permeameter specifically designed and calibrated for the characterization of porous insulation media [40]. The test specimens consist of insulation layers measuring 50 × 50 × 11–23 cm. All measurements are conducted under controlled laboratory conditions at 21 °C and 50 % relative humidity, corresponding to the ambient environment of the guarded hot box facility.

The measured effective air permeability values are presented in Fig. 3, alongside standard air permeability data obtained from independent external sources. A comparison of the datasets indicates that the results of the present study for the wood fiber insulation are in close agreement with those reported by other independent investigations [41]. The effective air permeability for wood wool at the density used in the wall element is estimated using exponential regression from the measurements performed on the material.

Similarly, the effective gas permeability for wood wool, other bio-based materials, and other common insulation materials can be seen in Fig. 3.

The effective gas diffusivity is measured, using oxygen as a tracer gas, with the Oxygen Diffusion Apparatus “ODA 20“ [42].

A summary of material properties of the loose-fill wood fiber insulation presently investigated can be found in [39].

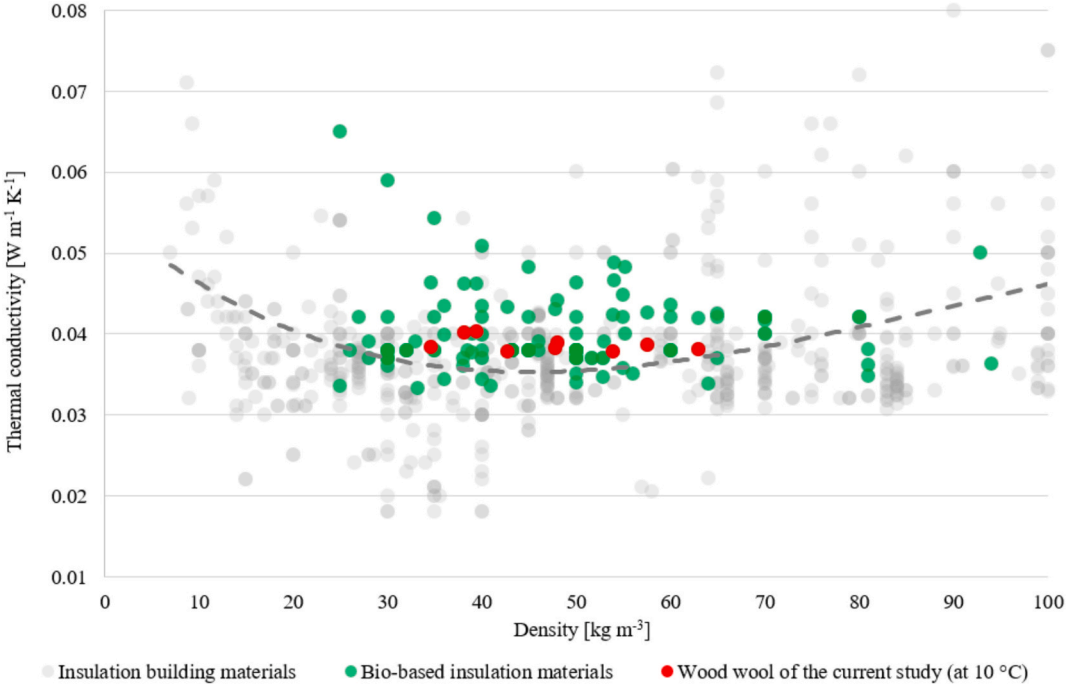

Fig. 2. Thermal conductivity as a function of the density for different insulation materials [39].

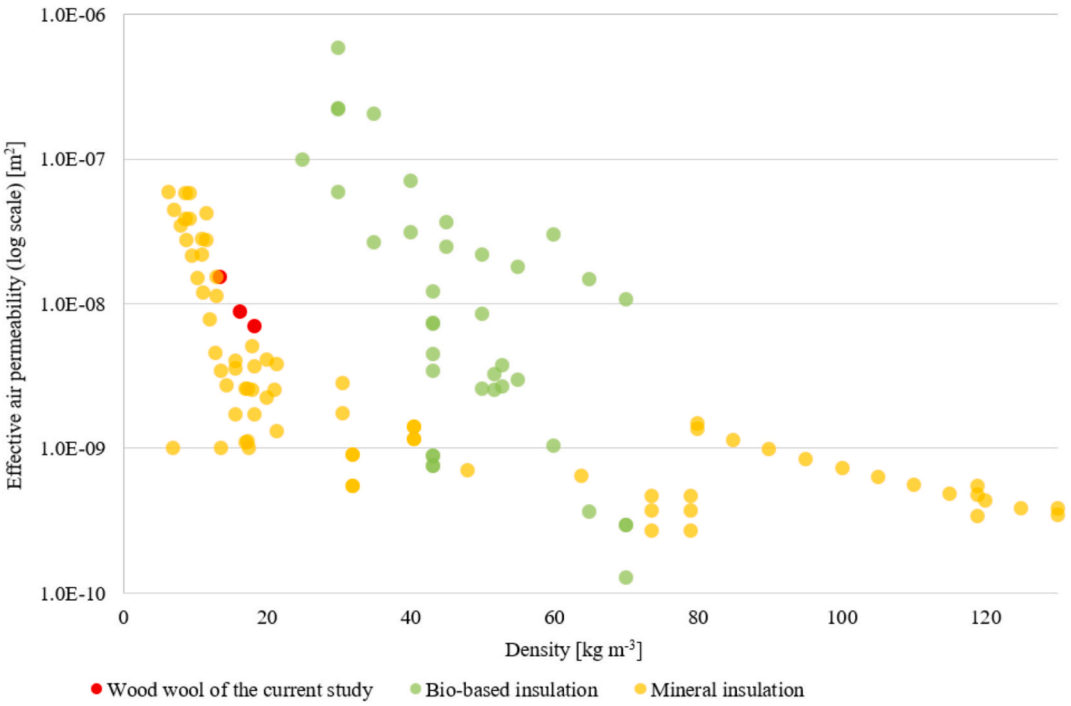

Fig. 3. Effective air permeability of different porous insulation materials [39].

2.2. Full-scale wall element

For the experiments, a full-scale wall element is constructed, with outer dimensions of 4.8 x 4.8 m, and internal dimensions of 3.6 x 3.6 m, with a total of 8 modules separated by construction wood. The wall element consists of loose-fill wood fiber insulation, construction wood, and orientated strand boards (OSB) plates. A horizontal cut of the modules is shown in Fig. 4, with the thermal properties of the materials in the wall element shown in Table 2. The wall element is tested without breather membranes or liners.

The temperature measurement points for the wall element are shown in Fig. 6.

3. Methodology

All experiments have been conducted in a guarded and calibrated hotbox with external dimensions of 4.8 x 4.8 m at the intersection between the hot and cold box, and internal dimensions of 3.6 x 3.6 m. A 3D rendering of the hot zone is shown in Fig. 5. The depth of the hot zone is 5.2 m.

The heat flux is measured from the hot zone to the cold zone with adiabatic conditions ensured elsewhere with a guarded zone. Parasitic heat losses to the sides of the specimen (such as heat loss to the laboratory) have been estimated during the calibration phase: keeping the temperature of the metering zone equal to that of the cold zone, but above the temperature in the environment surrounding the hotbox

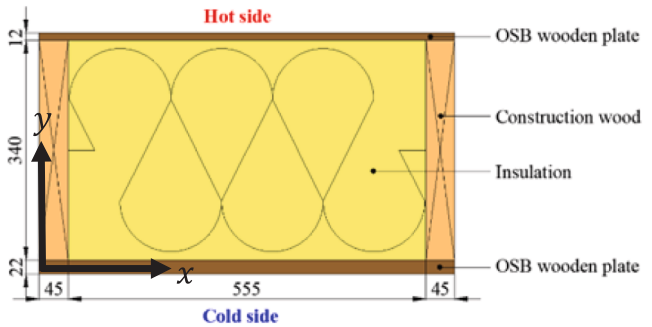

Fig. 4. Construction of a module in the wall element.

Table 2
Properties for each material in the wall element.[a]

Material	Thermal conductivity [W m^{-1} K^{-1}]	Density [kg m^{-3}]	Specific heat capacity [J kg^{-1} K^{-1}]
Wood fiber insulation	0.0382	43.42	1950
Construction wood	0.12	536	1200
OSB wooden plate	0.13	610/ 590*	1200

[a]Density for OSB plate for hot and cold side, respectively. [14–16].

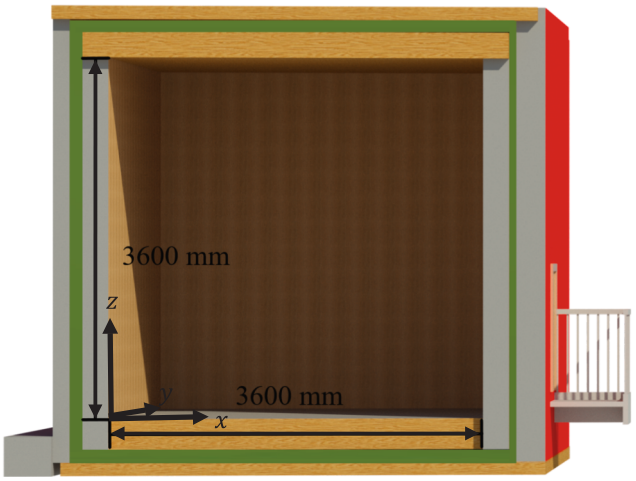

Fig. 5. 3D rendering of the hot zone of the hotbox. The light green area denotes the guarded zone. (For interpretation of the references to colour in this figure legend, the reader is referred to the web version of this article.)

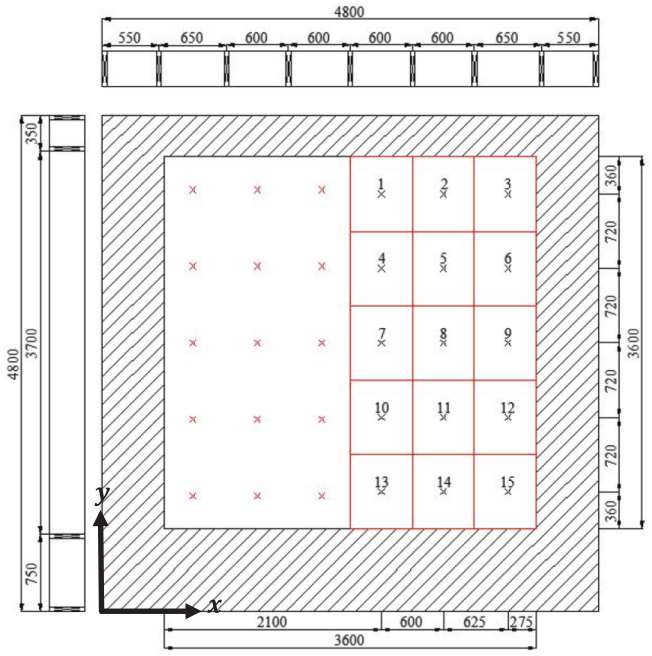

Fig. 6. Location of thermocouples on wall element. The black crosses are the placements, and the red crosses represent symmetry points, and the hatched area indicates the edge of the hotbox. All measurements are in millimeters. (For interpretation of the references to colour in this figure legend, the reader is referred to the web version of this article.)

setup.

The experiments have two different purposes: one is to determine the effective U-value of the wall element, and the second is to measure the internal temperature at different points of the insulation layer.

The effective U-value for steady-state experiments is determined using equation (3), while equation (4) is used for the determination of the effective U-value for dynamic experiments.

$$U = \frac{\Phi}{A(T_{ni} - T_{ne})} \tag{3}$$

Where U is the thermal transmittance, φ is the heat flow through the specimen, A is the surface area perpendicular to the heat flow, T_{ni} is the interior environmental temperature and T_{ne} is the exterior environmental temperature.

$$U = \frac{\sum_{j=1}^{n} Q_j}{A\sum_{j=1}^{n}\left(T_{ni,j} - T_{ne,j}\right)} \tag{4}$$

Where Q_j is the measured power, $T_{ni,j}$ is the interior environmental temperature and $T_{ne,j}$ is the exterior environmental temperature, where j refers to the j^{th} hour of the measurement.

A precision power meter measures the heat flux through the test sample (metering zone method). Hot-sphere anemometers measure the air velocity adjacent to the test sample, and thermocouples measured the surface temperatures of the surfaces in the hotbox and the cold box.

A total of 75 type-K thermocouples is placed inside the insulation material. The temperature is measured by thermocouples fastened on a fishing line with glue and thermo-shrinking tape, to ensure a precise placement of the thermocouple, so the thermocouple cannot move significantly in the depth of the insulation. The thermocouples are placed at five different heights in three different modules of the wall element. In each measurement point of the wall element, a total of five thermocouples are used to measure the temperature gradient inside the insulation. The macro-scale convection inside the insulation layer of the construction element would disturb the linear temperature distribution in the thickness of the element in steady-state conditions. The observation of non-linear temperature distribution in the thickness of the wall can thus indicate the presence of macro-scale convection cells inside the insulation layer (accounting for the boundary effects at the sides of the walls due to parasitic heat losses to the laboratory environment). On the outside of the wall element, thermocouples are used to measure the surface temperature and air temperature at the same measurement point as the thermocouples in the insulation material.

The measurement points for the thermocouples are shown in Fig. 6.

The thermocouples are placed on one side of the wall element, based on a symmetry assumption of the hotbox and wall element, where it is expected that the wall is homogenously affected by the boundary conditions on either side of the wall. A complete description of the experimental setup and considerations for other possible configurations for measurement points, mounting of thermocouples, etc, can be found in [36].

The equipment used in the experiment, with its ranges, accuracy, and purpose, is shown in Table 3.

A total of 11 cases of both steady-state and dynamic experiments are conducted (see Table 3 and Table 4). A description of the dataset, along with the dataset for the internal macro-scale convection measurements, can be found at [34] and [35], respectively. The steady-state experiments are conducted with different temperature differences, as the onset of internal macro-scale convection is directly proportional to the temperature difference. Each experiment is preceded by a stabilization phase (reaching steady state), followed by a minimum of 6 h of measurement recording, to make sure that the average value of the effective U-value during the latest 3 h deviates a maximum of 1 % from the previous 3 h.

Similarly, the dynamic cases are conducted until they have reached a quasi-steady state, meaning that the temperatures in the last 24 h do not deviate by more than 5 % compared to the temperatures at the same time for each measurement 24 h prior. The cold zone temperature follows a sinusoidal function for the dynamic cases, with a 24-hour period and 5 K or 10 K amplitude, respectively (see Table 5). Furthermore, an artificial sun was employed to add another boundary condition on the external surface of the test wall. For two of the dynamic tests, a constant irradiance of 628 W/m^2 was maintained between 10 am to 4 pm. Each dynamic case took 5 days to reach quasi steady state, for a total of 20 days of continuously running the guarded hot box with the full-scale wall element.

The phase shift in the cold box is estimated to be 0.85, such that the highest outdoor temperature occurs at 16:00 in the 24-hour measurement period, as this is typically where the highest temperatures occur in Denmark. This is used for the cases with irradiance, as the outdoor temperature and irradiance have to resemble a realistic condition.

To compare the effect of the internal macro-scale convection on the temperature gradients for different experiments, they are compared using a dimensionless number. They are compared with a theoretical calculation, such that the deviation from the theoretical value is attributed to other effects that are not considered in the calculation, like

Table 3
Overview of measurement equipment, as specified by the manufacturer.

Equipment	Purpose	Range	Accuracy
Type K thermocouples	Gas-phase and solid-phase measurements of the temperature	−70 to 270 °C	± 2.2 °C
Dantec hot-sphere anemometer	Local velocities close to wall element	0.05 to 5.0 m s^{-1}	> 1.0 m s^{-1}: ± 2 % ± 0.02 m s^{-1} > 1.0 m s^{-1}: ± 5 %
Power logger PEL 112	Measuring power output from heat source	Voltage: 10 to 1,000 V Current: 5 mA to 10 kA	Voltage: ± 0.2 % R ± 0.2 V Current: ± 0.3 %

Table 4
Overview of design temperatures pertaining to the steady-state cases.

Case	Indoor (warm) temperature [°C]	Outdoor (cold) temperature [°C]	Temperature difference [°C]
1	30	−20	50
2	20	−25	45
3	20	−20	40
4	20	−15	35
5	20	−10	30
6	20	0	20
7[a]	20	20	0

[a]Control case to investigate heat losses in guarded hotbox

Table 5
Overview of relevant parameters pertaining to the dynamic cases.

Case	Indoor (warm) temperature [°C]	Outdoor (cold) conditions		
		Mean temperature [°C]	Amplitude [°C]	Solar irradiance [W m^{-2}]
1	20	−10	10	0
2	20	−10	5	0
3	20	−10	10	628
4	20	−10	5	628

internal macro-scale convection. The dimensionless number can be seen in equation (5).

$$T_{dimensionless} = \frac{T_{measured} - T_{1D\ heat\ transfer}}{\Delta T_{experiment}} \quad (5)$$

Where $T_{dimensionless}$ is a dimensionless temperature, $T_{measured}$ is the measured temperature,

$T_{1D\ heat\ transfer}$ is a temperature calculated in each point based on the specified DS 418 calculation and $\Delta T_{experiment}$ is the temperature difference between the hot and cold side of the hot box, in each case.

3.1. Numerical setup

The numerical simulations were performed in COMSOL Multiphysics [43] to study the internal convection occurring within the loose-fill insulation. The goal of the numerical study was to compare numerical results with the experimental data, using a simulation case where the presence of internal convection is strictly controlled. The model represents a two-dimensional vertical section of the test element, with a height of 3.7 m and a thickness of 0.374 m. The insulation was modelled as a homogeneous porous domain, and an impermeable separator was introduced at the mid-plane to promote circulation within each half of the element. The separator was implemented as a zero-thickness internal boundary with no mass or heat transfer across it.

Two physics modules were used: Laminar Flow and Heat Transfer in Porous Media. The flow was assumed to be laminar and incompressible, and the governing equations were derived from the Navier-Stokes equations. The buoyancy-driven motion inside the porous medium was introduced through a volume force and acted as the driving mechanism for natural convection.

The heat transfer was computed using the assumption of local thermal equilibrium, meaning that the solid matrix and the fluid phase were considered to have the same temperature.

Fixed temperatures were applied at the hot and cold boundaries based on experimental surface measurements, while all other boundaries, including the separator, were treated as impermeable and adiabatic. No-slip conditions were applied to all solid interfaces.

The mesh was generated automatically and refined iteratively until grid-independent results were achieved. A stationary solver was employed to obtain steady-state velocity and temperature fields. The results were evaluated in terms of temperature distribution and airflow patterns inside the insulation and were compared directly with experimental temperature measurements at various heights and depths within the test element to assess model accuracy.

The effective thermal conductivity of the OSB wooden plates was adjusted to 0.03 W m^{-1} k^{-1} to bettter fit the experimental data.

4. Results and discussion

4.1. Temperature distribution in the steady-state cases

The results of the steady-state experiments show a significant deviation between the 1D heat transfer temperature gradient and the measured temperature gradient. This is consistent with previous studies that have found non-linear temperature gradients, which they attribute to internal macro-scale convection. All the steady-state case experiments show signs of internal macro-scale convection occurring in the insulation layer, as they all deviate from the theoretical calculation. The most significant case is the case with the largest temperature difference: case 1. The result from that case is shown in Fig. 7, where the temperature is shown as a function of the distance from the hot surface of the wall for different locations vertically in the wall. The placement of the thermocouples inside the wall element is shown below the temperature measurements. It is evident that the temperature gradient varies as a function of height, with the sensors at the top having a larger deviation from the theoretical calculation, which decreases for the sensors at the lower end of the wall element.

Only the sensors in the inner-most module with sensors are shown for clarity; however, the remaining sensors in the two other modules show similar trends. The temperature gradients in the height of the insulation are also investigated (see Fig. 8). For simple 1D heat transfer, a purely vertical temperature gradient is expected, meaning that the temperature is the same in the slice of the insulation. Fig. 8 shows that this is not the case, as the temperature gradients vary in the height of the insulation, most significantly at the bottom of the insulation. This could indicate that cold air is circulated downwards on the cold side of the insulation. The figure also shows that the boundary conditions, the temperature on the hot side and cold side, do not vary significantly with height.

As the case shown in Fig. 7 and Fig. 8 is an extreme case with a temperature difference of 50 °C. The results for case 6, which has a temperature difference of 20 °C, is shown in Fig. 9. One can see similar trends, with a slight deviation from the theoretical calculation, albeit significantly smaller. While the temperature profile on Fig. 7 had a similar deviation from the sensors at a height of 2.52 m and 3.24 m, the temperature profile at a height of 2.52 m is higher than that at 3.24 m when the temperature difference between the hot and cold sides is 20 °C. This could be due to a stronger convective flow at the higher temperature difference, while the lower temperature difference has a weaker convective flow, such that the flow changes direction before reaching the sensors at the top of the wall element.

The effect of internal macro-scale convection is visualized in Fig. 10, where the dimensionless temperature calculated using equation (5) is shown as a function of the depth of the insulation for different cases. As shown in Fig. 10, the dimensionless temperature profiles overall decrease in magnitude when the temperature difference decreases. It is assumed to be due to less internal macro-scale convection occurring, as the magnitude of the internal macro-scale convection is dependent on the temperature difference, as shown in equation (1). It should be noted that sensor error occurs in the case with a temperature difference of 35 °C at the surface temperature and air temperature sensor on the cold side, whereas the remaining sensors show similar tendencies as the other cases. The erroneous sensors have been removed on the plot. The cases with a temperature difference of 50 °C and 40 °C have been replicated and are shown with a dotted line.

To pursue the investigations, the effect of internal macro-scale convection is simulated with COMSOL Multiphysics modelling tool [43],

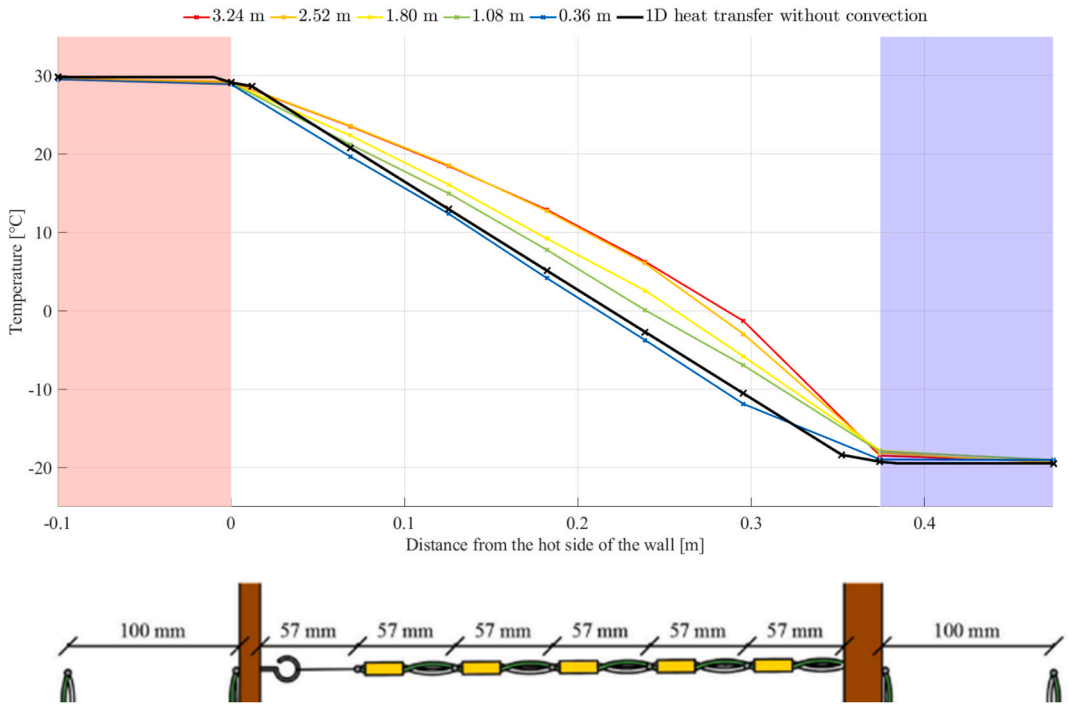

Fig. 7. Horizontal temperature profiles for a temperature difference of 50 °C in the specific heights. The variation of the temperature is smaller than the size of the markers.

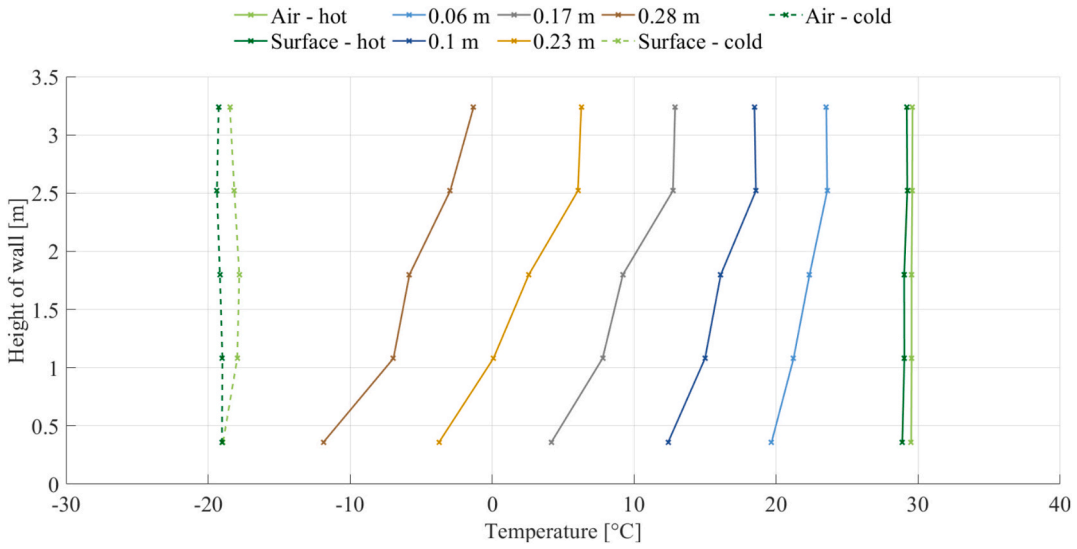

Fig. 8. Vertical temperature profiles for a temperature difference of 50 °C in the depth of the insulation layer for each column. The variation of the temperature is smaller than the size of the markers.

with the properties and boundary conditions of the experimental test cases. The modelled physics are laminar flow and heat transfer in porous media, where a volume force is added to control the macro convection and be compared to the experimental results. An impermeable barrier is placed in the middle of the wall element, to ensure that the air does not mix significantly and instead moves in a loop. Fig. 11 shows the results of the COMSOL simulation and experimental data, for the case of 50 °C temperature difference. The velocity vectors are shown on the COMSOL model to the right, as well as the internal impermeable barrier.

From Fig. 11, it can be concluded that a correspondence between the numerical simulation results and the experimental data is obtained in the middle of the construction element. The simulation data deviates from the experimental data at the top and bottom of the construction element, which can be due to how the volume force and impermeable barrier are implemented in the model. While the numerical results do not exhibit a strong fit to the experimental data, the overall temperature profiles have very similar trends when air movement is forced by a volume force inside the COMSOL model, which strengthens the hypothesis of internal macro-scale convection occurring in the insulation material.

4.2. *Temperature distribution in the dynamic cases*

Similarly, the results for the dynamic cases show a deviation between the theoretical temperature gradient and the measured temperature gradient. However, as the theoretical calculation does not include

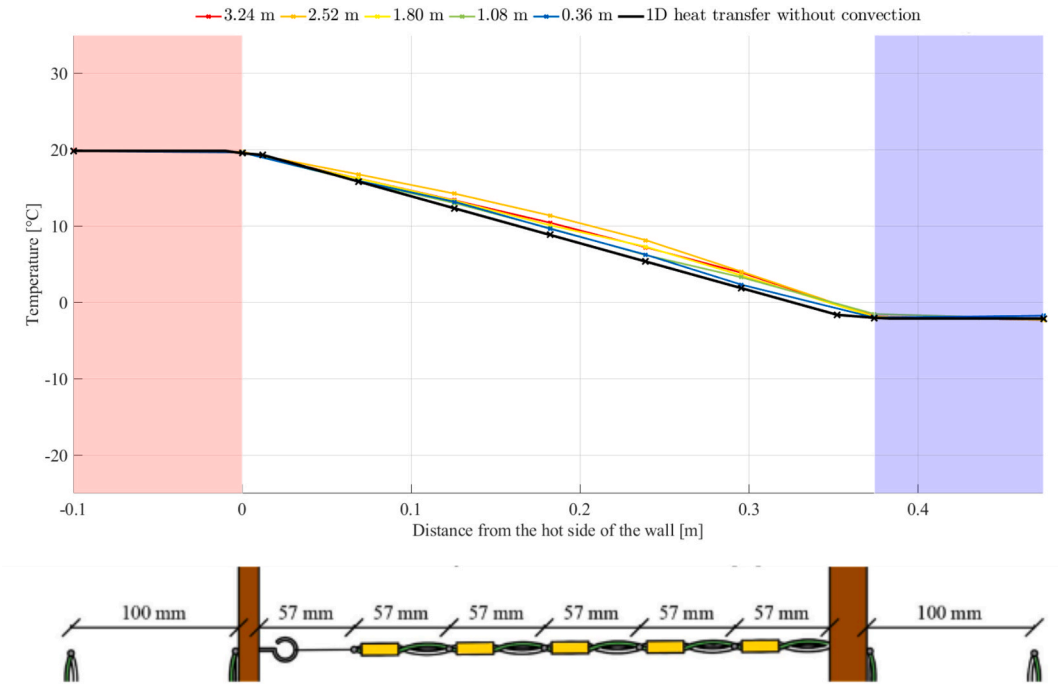

Fig. 9. Horizontal temperature profiles for a temperature difference of 20 °C in the specific heights at the highlighted column of the sensor placement (shown in the upper right corner). The variation of the temperature is smaller than the size of the markers.

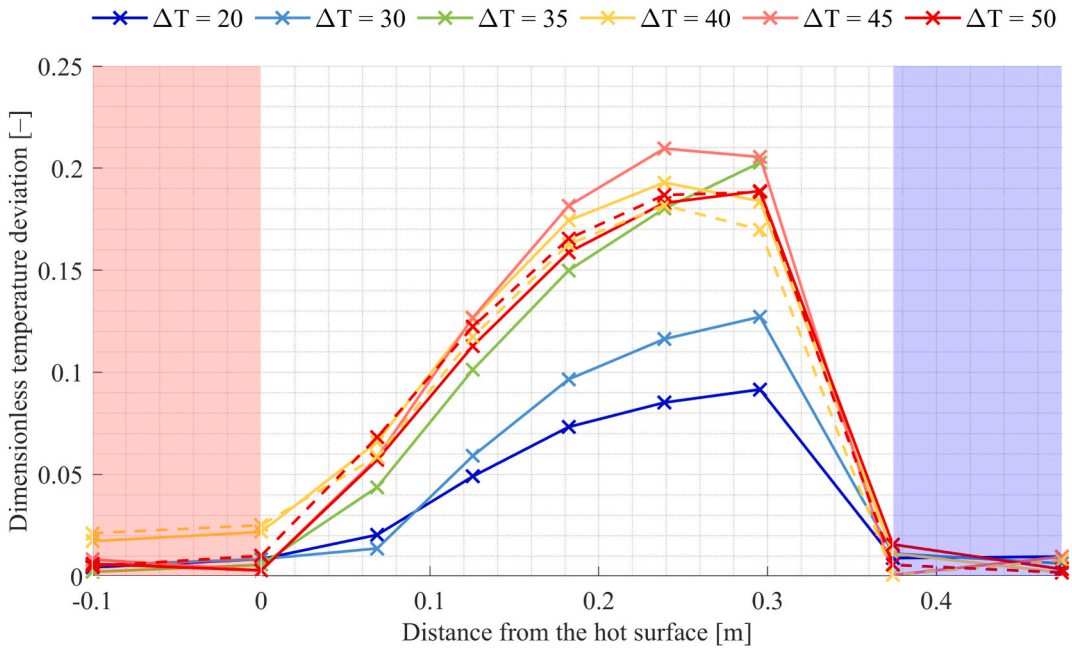

Fig. 10. Dimensionless temperature difference with DS 418 for the four steady-state cases at the highlighted point. Dotted lines are replicated cases of the cases with the corresponding colors.

thermal inertia, part of the deviation consists of the delayed response due to the temporal propagation of heat in the insulation layer. The results for case 1, with an amplitude of 20 °C, are shown in Fig. 12. This figure shows the dynamic behavior inside the insulation, as it shows the temperature deviation between sensors at the same depth of the insulation for a single module. This means that the temperature deviation between sensors in the top and bottom is changing, despite a temporal homogenously applied boundary condition on the entire wall. A temporal change in the temperature is expected due to the thermal mass of the insulation and the dynamic outdoor temperature. However, the temporal change should be homogeneous throughout the height of the insulation. With macro-scale internal convection, a more significant deviation occurs due to the movement of air. This effect is more pronounced on the cold side, as also shown in Fig. 11, where Fig. 12 shows the deviation for sensors across the height of the construction in each layer for a full 24-hour period.

As shown in Fig. 12, internal macro-scale convection occurs to a stronger extent with lower outdoor temperatures. The full extent of the macro-scale internal convection only occur a small amount of the total time. The internal temperature profile at two different times of the day is

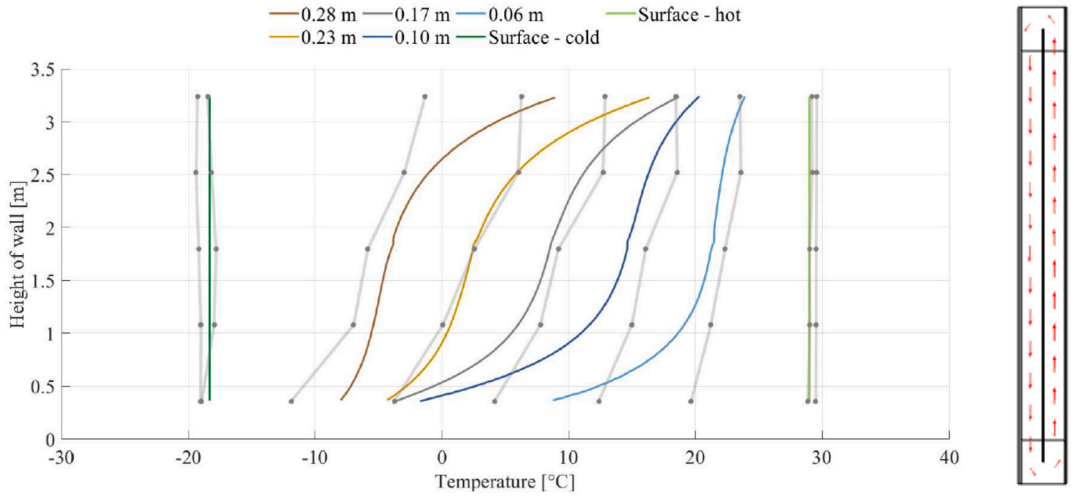

Fig. 11. Temperature profiles from COMSOL Multiphysics, with experimental data shown in grey. The model from COMSOL appears to the right with velocity vectors inside the insulation material.

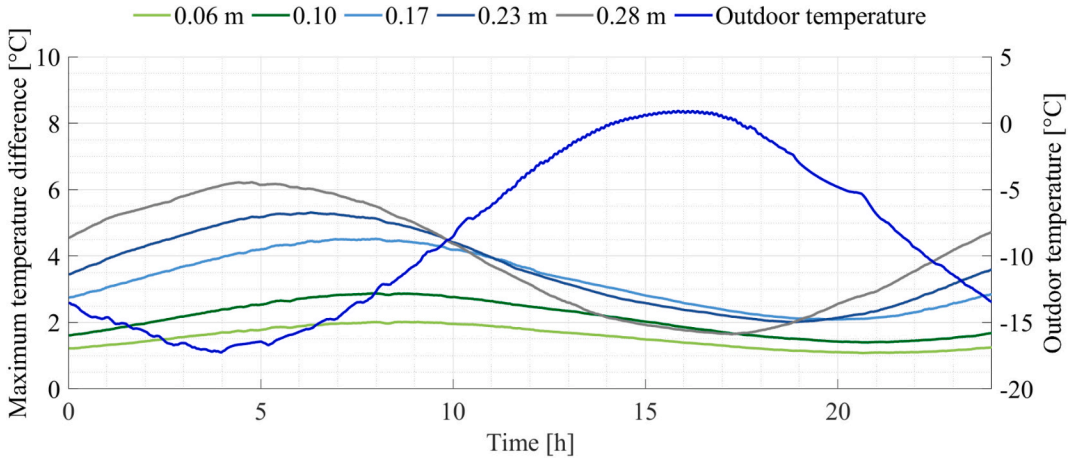

Fig. 12. Maximum temperature difference between sensors in the same depth of the construction as a function of time, for dynamic case 1. The measured distance starts from the hot side of the hotbox.

shown in Fig. 13, along with the outdoor temperature in the 24-hour period. A similar calculation is performed in COMSOL Multiphysics, which includes the thermal inertia of the insulation material, but not the internal macro-scale convection. When the temperature is at its highest, the temperature gradients have a smaller deviation than the one calculated in COMSOL Multiphysics, which could be due to internal macro-scale convection increasing the temperature. This indicates that there is an additive nature between thermal inertia and internal macro-scale convection.

The extreme case shown in Fig. 13 is not representative of the Danish weather conditions, therefore, a less extreme case is also investigated. Case 2 is shown in Fig. 14.

As shown in Fig. 14, the dynamic case with a mean outdoor temperature of −5 °C shows that the effect of internal macro-scale convection is lower than the steady-state case with an outdoor temperature of −10°C. The less pronounced effect of internal macro-scale convection in dynamic conditions could be due to the thermal inertia of the insulation material, meaning that it delays the temporal propagation of heat, resulting in a lower temperature difference and, therefore, worse conditions for internal macro-scale convection to occur.

4.3. *Measurements of the effective U-value*

The effect of internal macro-scale convection is clearly visible inside the insulation. As it is assumed to cause an additional heat loss, it should have a clear impact on the effective U-value, with a larger temperature difference yielding a higher U-value due to the additional heat loss. This is investigated using equation (3) for the steady-state cases. The results of the effective U-value are shown in Fig. 15.

As shown in Fig. 15, a larger temperature difference yields a higher measured U-value. There is a linear tendency, meaning that the modified Rayleigh number, which is used to predict the onset of internal macro-scale convection, also indicates that the magnitude of the internal macro-scale convection is linearly proportional to the temperature difference, except in the dynamic experiments with sun. However, this is expected, as the solar radiation adds solar gains which decreases the estimated effective U-value.

The modified Nusselt number, calculated using equation (2), is normalized by the lowest Nusselt number and shown as a function of the modified Rayleigh number, see Fig. 16. After the onset of internal macro-scale convection, there should be an increasing linear tendency [44,45], which is confirmed in the figure. Due to the linear trend, it can be concluded that internal macro-scale convection was exhibited in all tests, to varying degrees. With lower temperature differences between

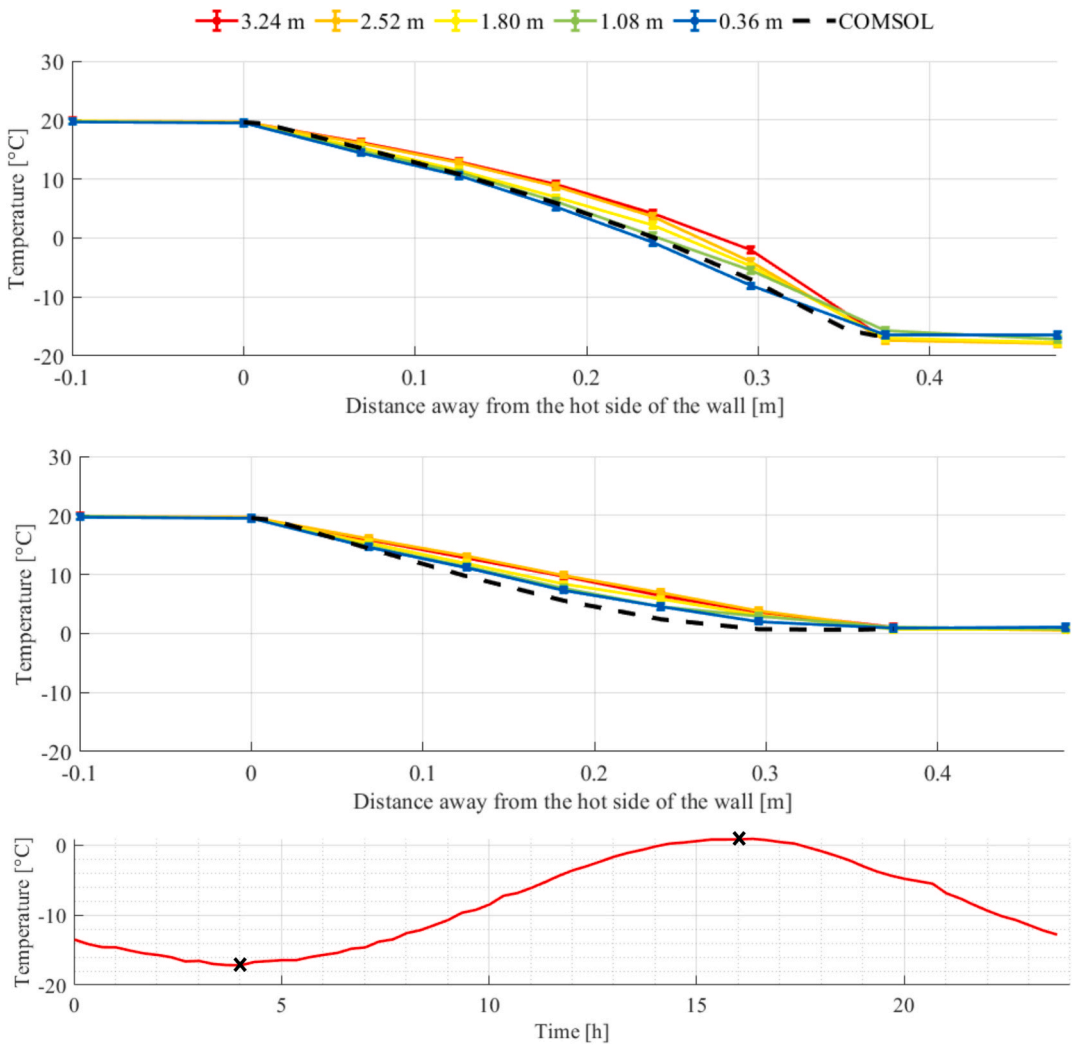

Fig. 13. Horizontal temperature profiles for case 1. The black crosses illustrate the time and temperature for which the temperature profile in the wall element is determined. Upper) Hour 4. Lower) Hour 16.

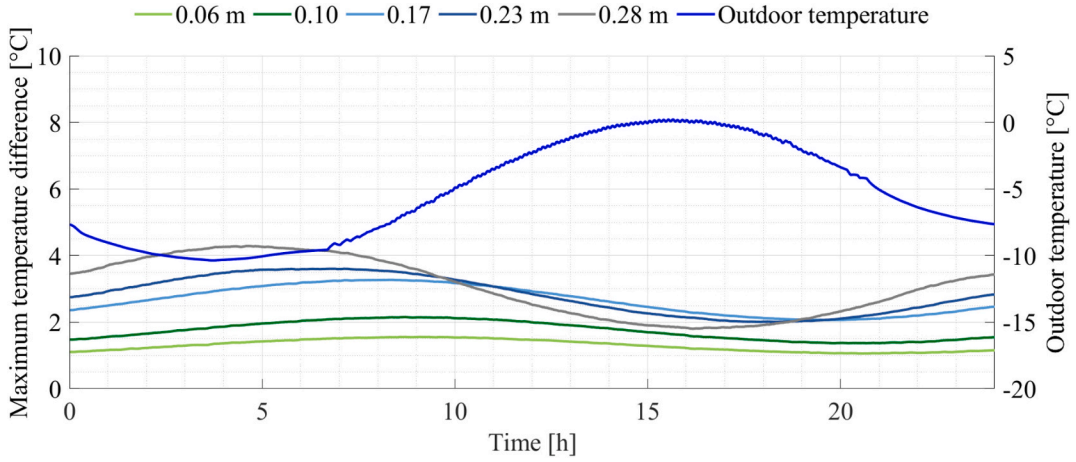

Fig. 14. Maximum temperature difference between sensors in the same depth of the construction as a function of time, for dynamic case 2. The measured distance starts from the hot side of the hotbox.

the hot and cold sides of the guarded hotbox, the normalized Nusselt number should be constant, as a function of the modified Rayleigh number. Since this is not exhibited in Fig. 16, the critical Rayleigh number for this setup cannot be determined.

5. Conclusions and suggestions for future work

The objective of the study was to investigate the presence of macro-scale internal macro-scale convection in loose-fil wood fiber insulation

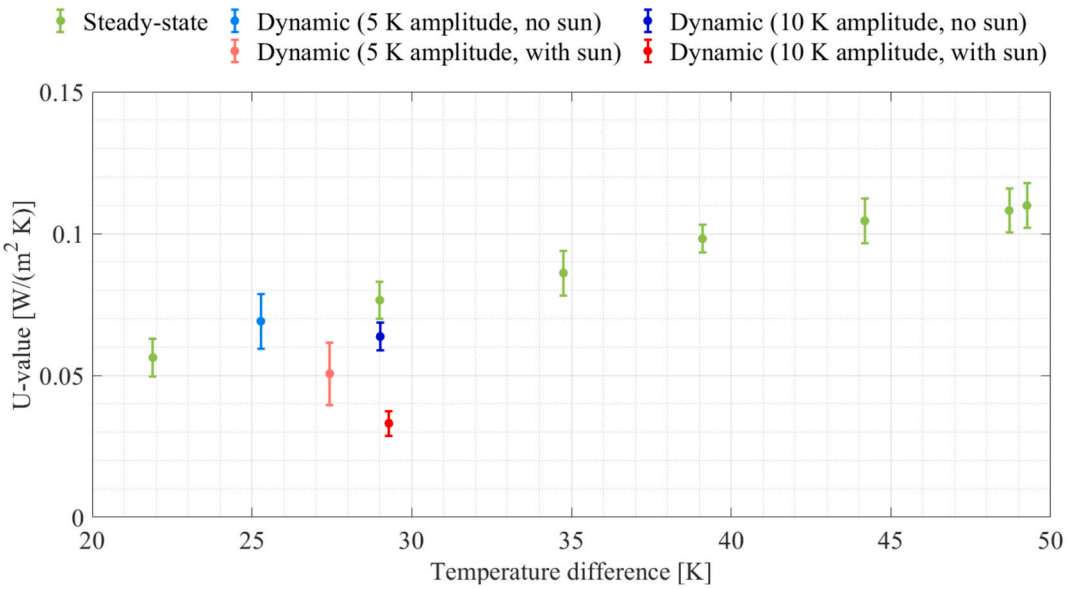

Fig. 15. Effective U-value measurements as a function of temperature difference between the cold and the warm side of the wall, for both steady-state and dynamic cases. The error bars indicate the uncertainty of the measurement (sensor calibration and parasitic heat losses from the hotbox setup).

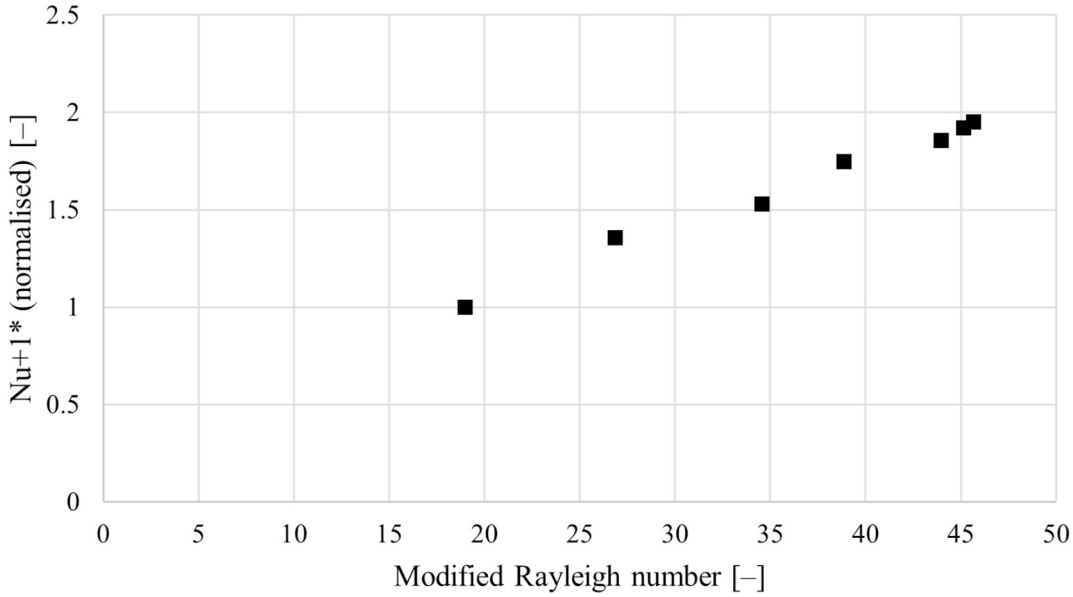

Fig. 16. Normalised Nusselt number as a function of the modified Rayleigh number for static experiments.

in a vertical wall, and its impact on the effective U-value in steady-state and dynamic conditions. Observations of the measured temperature gradients in the insulation material indicate that internal macro-scale convection occurs in the investigated wood fiber insulation in both steady-state and dynamic conditions. A clear trend of internal macro-scale convection increasing linearly with the increasing temperature difference was shown. The effective U-value similarly showed an increasing tendency of a higher U-value with increasing temperature differences, indicating that at higher temperature differences, additional losses occur. The additional losses from internal macro-scale convection are significant. It was shown that cases with higher temperature differences experience a higher effective U-value, due to the extra heat transfer from the internal macro-scale convection. The U-value increased more than 90 %, when considering the case with the lowest and highest temperature difference at steady-state between the hot and cold side. Due to this significant increase in heat losses for loose-fill wood fiber insulation, internal macro-scale convection cannot be ignored at high temperature differences between ambient and outdoor conditions. However, due to the mild climate of Denmark, the effects of internal macro-scale convection are not significant, as the results showed that a high temperature difference is needed for it to be significant, with the effect being even less prominent in dynamic conditions. The temperature difference between ambient and outdoor conditions is often around 20 °C for a large part of the year, with some exceptions during cold winters. Since no critical Rayleigh number could be identified, it is difficult to assess exactly when the onset of internal macro-scale convection occurs, and consequently what the expected increase in U-value would be.

While no control case was conducted with an insulation material that has little or no air permeability, this should be considered in future studies to ensure that the effect on the temperature profiles exhibited in this study is not due to other factors. Furthermore, the insulation in the

wall element in this study was installed by professionals, meaning that the insulation was blown in as it would be on a real wall element. However, this could introduce non-homogenous fiber networks in the wall-element, that could potentially influence the temperature profiles in the wall-element. Future work could look into the effect of these, and how they can affect the internal convection in the insulation.

The numerical simulation carried out in COMSOL Multiphysics showed similar temperature gradients and distributions as in the experimental data. It deviated at the top and bottom of the construction element, which could be improved by changing the size of the impermeable barrier or changing how and where the volume force is implemented. The air movement inside the insulation in the numerical simulation was forced by a volume force and not a product of the modeled physics. More work should be done in modeling the air movement in porous media, which could be done using Darcy's Law or Brinkmann's Law, which could shed light on what works best when simulating internal macro-scale convection in a building physics context.

Finally, instead of observing the effects of internal macro-scale convection, it could be measured more directly by using different methods to confirm or deny whether the air movement inside the insulation material is the cause of the non-linear temperature gradients. Different methods could be utilized, such as injecting tracer gas at the bottom of the hot side of the insulation and measuring the amount of tracer gas in the air at the top of the hot side of the insulation. This could be used to estimate the air velocity of the air movement or indicate that air is not moving inside the insulation. More direct approaches, such as using anemometers, are deemed unfit for this type of investigation, due to the low velocity of the air movement, along with heat generation from certain anemometers, such as hot-sphere anemometers, and the difficulties with mounting the anemometers in the insulation material without disturbing the heat transfer.

CRediT authorship contribution statement

Martin Veit: Writing – original draft, Visualization, Software, Investigation, Data curation. **Hicham Johra:** Writing – review & editing, Visualization, Supervision. **Nikolaj Rask:** Writing – original draft, Investigation. **Simon M. Roesgaard:** Writing – original draft, Visualization, Conceptualization. **Rasmus Lund Jensen:** Writing – review & editing, Supervision.

Declaration of competing interest

The authors declare that they have no known competing financial interests or personal relationships that could have appeared to influence the work reported in this paper.

Acknowledgements

The authors would like to express their gratitude to Thermocell A/S [https://thermocell.dk], for providing the bio-based loose-fill wood fiber insulation material.

Data availability

Data will be made available on request.

References

[1] European Parliament and Council, Directive 2010/31/EU of the European parliament and of the Council of 19 May 2010 on the energy performance of buildings, Off. J. Eur. Union (2010) 13–35.
[2] P.D. Wilde, The gap between predicted and measured energy performance of buildings: a framework for investigation, Autom. Constr. (2014), https://doi.org/10.1016/j.autcon.2014.02.009.
[3] S Pallin, J DeGraw, M Bhandari and T Pilet, Quantifying Thermal Performance of the Building Envelope - Beyond Common Practice, in: Current Topics and Trends on Durability of Building Materials and Components, Serrat, C., Casas, J.R. and Gibert, V. doi: 10.23967/dbmc.2020.204.
[4] Veit M, Johra H, Jensen R L, Rask N and Roesgaard S M. (2023a). Numerical sensitivity analysis of the energy performance of building envelope with dynamic conditions. Journal of Physics: Conference Series, Volume 2654, Proceedings of the 13th Nordic Symposium on Building Physics (NSB-2023). 12-14 June 2023. Aalborg, Denmark. https://doi.org/10.1088/1742-6596/2654/1/012109.
[5] Veit M, Johra H. (2023b). A comparative study of BSim and COMSOL Multiphysics for steady-state and dynamic simulation of transmission loss. DCE Technical Reports Nr. 309, Aalborg University. https://doi.org/10.54337/aau518779357.
[6] F. Déqué, F. Ollivier, J. Roux, Effect of 2D modelling of thermal bridges on the energy performance of buildings, Energ. Buildings 33 (6) (2001) 583–587, https://doi.org/10.1016/s0378-7788(00)00128-6.
[7] DS 418, 2011. DS 418. Calculation of heat loss from buildings. Danish Standard, 7. edition, 2011.
[8] C. Bankvall, Heat transfer in insulation and insulated structure, Div. of Building Technology, Lund Institute of Technology, 1972.
[9] Iso, 10456. Building materials and products - Hygrothermal properties - Tabulated design values and procedures for determining the declared and design thermal values, Danish Standard 2 (2008) Edition.
[10] K.E. Wilkes, J.L. Rucker, Thermal performance of residential attic insulation, Energ. Buildings 5 (4) (1983) 263–277, https://doi.org/10.1016/0378-7788(83)90014-2.
[11] A. Silberstein, C. Langlais, E. Arquis, Natural Convection in Light Fibrous Insulating Materials with Permeable Interfaces: Onset Criteria and its effect on the thermal Performances of the product, J. Therm. Insul. (1990), https://doi.org/10.1177/109719639001400104.
[12] R. Arambakam, T. Hooman, B. Pourdeyhimi, Modeling performance of multi-component fibrous insulations against conductive and radiative heat transfer, Int. J. Heat Mass Transf. 71 (2014) 341–348, https://doi.org/10.1016/j.ijheatmasstransfer.2013.12.031.
[13] H. Johra, P. Léard (2025). Large-scale experimental investigations on the critical Rayleigh number for internal natural convection inside blown glass wool. Proceedings of the Finnish Building Physics Conference 2025, The newest research results and good practical solutions, Proceedings 9. Tampere, Finland, October 28-29.
[14] C. Langlais, E. Arquis, D. McCaa, A Theoretical and Experimental Study of Convective Effects in Loose-Fill thermal Insulation. Insulation Materials, Testing and applications, in: D. McElroy, J. Kimpflen (Eds.), 100 Barr Harbor Drive, PO Box C700, ASTM International, West Conshohocken, PA 19428–2959, 1990.
[15] M. Serkitjis, Natural convection heat transfer in a horizontal thermal insulation layer underlying an air layer. Proceedings of the 2nd International Conference on Building Physics, 1995.
[16] M. Serkitjis, P. Wahlgren, C.E. Hagentoft (2001). Natural and Forced Convection in a Superposed Air and Porous Layer when Heated from Below. In Proceedings of the 5th World Conference on Experimental Heat Transfer, Fluid Mechanics and Thermodynamics (ExHFT-5). Thessaloniki, Greece.
[17] P. Wahlgren, Measurements and Simulations of Natural and Forced Convection in Loose-Fill attic Insulation, J. Therm. Envelope Build. Sci. 26 (1) (2002) 93–109, https://doi.org/10.1177/0075424202026001116.
[18] P. Wahlgren (2004). Convection in Loose-fill Attic Insulation–Simulations and Large-scale Measurements. In Proceedings of the 9th Conference on the Thermal Performance of the Exterior Envelopes of Whole Buildings. Clearwater Beach, Florida, USA.
[19] C. Ciucasu, J. Gilles, E. Montoya, E. Arquis (2005). Convection phenomena in loose-fill attics. In Proceedings of the 7th Symposium on Building Physics in the Nordic Countries. Reykjavik, Iceland. page 13-15.
[20] P. Wahlgren (2005). Variation in critical modified Rayleigh number in porous attic insulation due to geometry and materials. In Proceedings of the 7th Symposium on Building Physics in the Nordic Countries. Reykjavik, Iceland.
[21] A.A. Delmas, K.E. Wilkes (1992). Numerical analysis of heat transfer by conduction and natural convection in loose-fill fiberglass insulation–effects of convection on thermal performance. Technical Report, Oak Ridge National Lab. (ORNL), Oak Ridge, TN (United States), U.S. Department of Energy. ORNL/CON-338; ON: DE92014938. https://doi.org/10.2172/10147925.
[22] A.A. Delmas, E. Arquis, Early Initiation of Natural Convection in an Open Porous Layer due to the Presence of Solid Conductive Inclusions, ASME Journal of Heat and Mass Transfer 117 (3) (1995) 733–739, https://doi.org/10.1115/1.2822637.
[23] S. Uvsløkk, H.B. Skogstad, S. Grynning, How to prevent natural convection causing extra heat loss and moisture problems in thick insulation layers, Passivhus Norden, 2010.
[24] P.J. Burns, L.C. Chow, C.L. Tien, Convection in a vertical slot filled with porous insulation, Int. J. Heat Mass Transf. 20 (9) (1977) 919–926, https://doi.org/10.1016/0017-9310(77)90062-X.
[25] L. Gullbrekken, S. Uvsløkk, T. Kvande, B. Time, Hot-Box Measurements of Highly Insulated Wall, Roof and Floor Structures, Sage Publishing, 2016, 10.1177/1744259116669516.
[26] L. Gullbrekken, S. Grynning, J.E. Gaarder, Thermal performance of insulated construction, SNTEF Building and Infrastructure (2019), https://doi.org/10.3390/buildings9020049.
[27] S. Dyrbøl, S. Svendsen, A. Elmroth, Experimental investigation of the effect of natural convection on heat transfer in mineral wool, J. Therm. Envelope Build. Sci. 26 (2) (2002) 153–164, https://doi.org/10.1177/0075424202026002930.

[28] P. Wahlgren (2004). Convection in loose-fill attic insulation - Measurements and numerical simulations, in: Performance of Exterior Envelopes of Whole Buildings IX International Conference, Clearwater Beach, 2004.
[29] P. Wahlgren, Overview and Literature Survey of natural and forced convection in attic insulation, J. Build. Phys. 30 (4) (2007) 351–370, https://doi.org/10.1177/1744259106075947.
[30] Ciucasu, C. Gilles, J., Ober, D., Petrie, T., Arquis, E. (2006). Convection phenomena in loose-fill attics - Tests and simulations.
[31] H. Kivioja, J. Vinha, Hot-box measurements to investigate the internal convection of highly insulated loose-fill insulation roof structures, Energ. Buildings 216 (2020) 109934, https://doi.org/10.1016/j.enbuild.2020.109934.
[32] B.L. Jensen, M. Pedersen, L. Olsen, Alternativ isolering – undgå byggeskader, Danish Technological Institute. (2004).
[33] L. Ikatti, Bestämning av sättning vid vibration lösfyllnadsisolering av träull, Sveriges Tekniska (2016). Forskningsinstitut.
[34] Veit M, Johra H. (2023c). Temperature measurements of full-scale wall element using Type K thermocouples to observe internal convection in loose-fill wood fiber insulation. DCE Technical Reports Nr. 317, Aalborg University. doi: 10.54337/aau544775163.
[35] M. Veit, H. Johra, Temperature measurements of full-scale wall element using Type K thermocouples to observe internal convection in loose-fill wood fiber insulation, Zenodo (2023).
[36] Veit M, Johra H. (2022). Experimental Investigations of a Full-Scale Wall Element in a Large Guarded Hot Box Setup: Methodology Description. DCE Technical Reports Nr. 304, Aalborg University. doi: 10.54337/aau488363266.
[37] K.R. Jensen, P. Fojan, R.L. Jensen, L. Gurevich, Water condensation: a multiscale phenomenon, J. Nanosci. Nanotechnol. 14 (2) (2014) 1859–1871, https://doi.org/10.1166/jnn.2014.9108.
[38] H. Johra (2019). Description of the Guarded Hot Plate Method for Thermal Conductivity Measurement with the EP500. DCE Lecture Notes No. 75. Aalborg University, Department of Civil Engineering. https://doi.org/10.54337/aau317020205.
[39] Johra H (2019). Thermal properties of common building materials. DCE Technical Reports No. 216. Aalborg University, Department of Civil Engineering. https://vbn.aau.dk/ws/portalfiles/portal/294603722/Thermal_properties_of_common_building_materials.pdf.
[40] H. Johra, Air Permeameter for Porous Building Materials: Aalborg University Prototype 2023. DCE Lecture Notes, No. 84, Aalborg University, Department of the Built Environment, 2023.
[41] H. Johra, Thermal Properties of Building Materials - Review and Database. DCE Technical Reports, Nr. 289, Department of the Built Environment, Aalborg University, 2021.
[42] K.M. Frandsen, Y.I. Antonov, H. Johra, P. Møldrup, R.L. Jensen, Experimental Investigation of Water Vapor Diffusivity in Bio-Based Building Materials by a Novel Measurement Method, United Kingdom, Cambridge, 2021.
[43] COMSOL. COMSOL Multiphysics Simulation Software. https://www.comsol.com, 2022.
[44] D.A. Nield, A. Bejan, Convection in Porous Media, Fifth Edition, Springer, 2017, 10.1007/978-3-319-49562-0.
[45] S. Bories (1987). Natural convection in porous media. In J. Bear et al. (eds.), Advances in Transport Phenomena in Porous Media. NATO ASI Series E: Applied Sciences - No. 128. Martinus Nijhoff Publishers, Dordrecht. https://doi.org/10.1007/978-94-009-3625-6.